This manuscript was accepted by J. Chem. Phys. Click here to see the version of record.

Fluctuation Correction for the Critical Transition of Symmetric Homopolymer Blends

Thomas M. Beardsley and Mark W. Matsen*

Department of Chemical Engineering,

Department of Physics & Astronomy,

and Waterloo Institute for Nanotechnology,

University of Waterloo, Waterloo, Ontario, Canada

(Dated: July 7, 2017)

Abstract

Monte Carlo simulations are performed on structurally symmetric binary homopolymer blends over a wide range of invariant polymerization indexes, $\bar{N}$. A finite-size scaling analysis reveals that certain critical exponents deviate from the expected 3D-Ising values as $\bar{N}$ increases. However, the deviations are consistent with previous simulations, and can be attributed to the fact that the system crosses over to mean-field behavior when the molecules become too large relative to the size of the simulation box. Nevertheless, the finite-size scaling techniques provide precise predictions for the position of the critical transition. Using a previous calibration of the Flory-Huggins interaction parameter, χ, we confirm that the critical point scales as $(\chi N)_c = 2 + c\bar{N}^{-1/2}$ for large $\bar{N}$, and more importantly we are able to extract a reliable estimate, $c \approx 1.5$, for the universal constant.

This manuscript was accepted by J. Chem. Phys. Click here to see the version of record.

I. INTRODUCTION

The theory of binary homopolymer blends developed by Flory[1] and Huggins[2] has long been a standard topic of polymer textbooks; see Ref. 3 for a recent review. The focus is typically on structurally symmetric blends involving polymers of the same molecular volume, $v_m = N/\rho_0$, and average end-to-end length, $R_0 = aN^{1/2}$, where ρ_0^{-1} is the segment volume, N is the number of segments in each polymer, and a is the statistical segment length. For blends of 50:50 composition, the onset of macrophase separation is predicted to occur at a critical point of $(\chi N)_c = 2$, where χ is the usual Flory-Huggins interaction parameter.

The Flory-Huggins theory corresponds to the mean-field approximation of the standard incompressible Gaussian chain model (GCM), upon which most calculations in polymer theory are based.[4,5] Renormalized one-loop (ROL) expansions of the model[6–8] have shown that the mean-field predictions are exact in the infinite molecular-weight limit, and that deviations for large finite polymers depend on the ratio $R_0^3/v_m = \bar{N}^{1/2}$, where $\bar{N} \equiv a^6\rho_0^2 N$ is referred to as the invariant polymerization index. A recent ROL calculation by Qin and Morse[9] predicts

$$(\chi N)_c = 2 + c\bar{N}^{-1/2} \ , \tag{1}$$

with $c = 3.7$. The fluctuation correction to mean-field theory is believed to be universal, but ROL is not expected to provide an accurate estimate of its size, c. The problem is that the ROL calculation breaks down near the critical point, because it fails to treat the critical fluctuations properly.

The most straightforward way of accounting for fluctuations is by performing simulations. A recent simulation by Detcheverry *et al.*[10] has found clear evidence of the $\bar{N}^{-1/2}$ scaling, but with a coefficient, $c \approx 10$, that is nearly three times the ROL prediction. Technically speaking, however, it is impossible to directly simulate the GCM, where chains are treated as one-dimensional elastic threads with zero-range interactions, and consequently Detcheverry *et al.* were forced to approximate the GCM. One way to circumvent this problem is to mathematically transform the GCM into an equivalent field-based model, which just involves two fields governed by an appropriate Hamiltonian.[11] The fluctuating fields can then be simulated on a three-dimensional grid. Spencer and Matsen[12] performed a field-theoretic simulation (FTS) of this type last year and found reasonable agreement with the $\bar{N}^{-1/2}$ scaling. However, this time, the coefficient was approximately half the size of the ROL

prediction.

Since the $\bar{N}^{-1/2}$ fluctuation correction is supposedly universal, it should hold for any model, including the bond-fluctuation model (BFM) simulated by Deutsch and Binder[13] 25 years ago. They located critical points for two variants of the BFM, using accurate finite-size scaling techniques. Given that the simulations were for a lattice model as opposed to the standard GCM, comparison to Eq. (1) is contingent upon the definition of an effective χ parameter. Naturally, it must satisfy the requirement that $(\chi N)_c \to 2$ as $N \to \infty$.

Müller and Binder[14] proposed the definition $\chi = z(N)\alpha$, where α is the interaction energy between unlike monomers compared to like monomers in units of k_BT and $z(N)$ is the average number of intermolecular contacts a monomer experiences in the athermal limit (*i.e.*, $\alpha \to 0$). Using this definition, Müller[15,16] showed that both variants of the BFM produced consistent results with $c \approx 4$, which is close to the ROL prediction. However, Qin and Morse[9] pointed out that this definition of χ depends on the size of the molecules, N, which contradicts our expectation that χ should depend solely on the interactions between monomers and not on quantities related to the architecture of the molecules. With this in mind, they reanalyzed the BFM simulations using the definition $\chi = z_\infty\alpha$, where $z_\infty = \lim_{N\to\infty} z(N)$. When doing so, the fluctuation correction turned out to be very small and showed no signs of universality nor the expected $\bar{N}^{-1/2}$ scaling. Qin and Morse suggested the problem might be because χ should, in fact, be a nonlinear function of α, which only reduces to $\chi \approx z_\infty\alpha$ for small α.

The justification for using a nonlinear χ has now been nicely illustrated in simulations of symmetric diblock copolymer melts by Morse and coworkers.[18,19] Their calibration of $\chi(\alpha)$ was obtained by matching the disordered-state structure function, $S(q)$, of the simulations to that of ROL under the constraint $\chi(\alpha) \to z_\infty\alpha$ in the athermal limit. When expressed in terms of the nonlinear χ, the order-disorder transitions, $(\chi N)_{\mathrm{ODT}}$, from five distinct simulation models reduced to a universal function of $\bar{N}$. With this improved way of defining χ, simulations have now been able to accurately predict experimental results.[20]

Here, we attempt to determine an accurate value of the coefficient, c, in Eq. (1) with simulation. Given that c is universal, there is no need to choose a physically realistic model. Therefore, we select the lattice model originally introduced by Vassiliev and Matsen.[21] Not only is it extraordinarily simple, the model has already been accurately calibrated in Ref. 18. Therefore, we just need to locate the critical points for a series of different chain lengths, which we do following a similar finite-size scaling analysis to that of Deutsch and Binder.[13]

III. SIMULATION METHOD

This section describes our Monte Carlo simulation for a binary blend of n_A A-type and n_B B-type polymers, each consisting of N beads (or monomers). To simplify the simulation, the polymers are restricted to a periodic fcc lattice with a maximum of one monomer per lattice site and bonded monomers occupying nearest-neighbor sites. The fcc lattice is created by taking a simple-cubic $L \times L \times L$ lattice and deleting every second site. For convenience, the nearest-neighbor spacing, b, is set to $2^{1/6} = 1.122$, such that the volume of the system, V, equals the total number of lattice sites, $L^3/2$. To allow room for the polymers to move, the lattice is only filled to a monomer density of $\rho_0 \equiv nN/V = 0.8$, where $n = n_A + n_B$. Molecular interactions are limited to neighboring A and B monomers, for which the interaction energy is $\epsilon_{\rm AB}$.

This model has already been accurately calibrated in Ref. 18 from a simulation on diblock copolymer melts. From that, we know that its statistical segment length is $a = 1.233b = 1.384$, which implies $\bar{N} = 4.506N$. Furthermore, the study found that the Flory-Huggins interaction parameter is well approximated by

$$\chi(\alpha) = \frac{z_\infty \alpha + c_1 \alpha^2}{1 + c_2 \alpha} \ , \tag{2}$$

where $\alpha \equiv \epsilon_{\rm AB}/k_BT$ and $z_\infty = 4.897$ was determined by evaluating the number of intermolecular contacts at $\alpha = 0$. The fitting parameters, $c_1 = 88.5$ and $c_2 = 8.30$, were obtained by matching the peak in the structure function, $S(q^*)$, from the simulation to that of ROL across the entire disordered phase for seven different chain lengths ranging from $N = 20$ to 180.

Our current simulation on a binary homopolymer blend is performed in a semi-grand canonical ensemble, where the total number of molecules is fixed but the difference, $m = (n_A - n_B)/n$, is permitted to fluctuate. This is done by allowing each molecule to swap between types A and B. In addition, the molecules can also move by undergoing slithering snake and crankshaft steps.[21] The swap, slithering snake and crankshaft moves are attempted with relative frequencies of $3/N$:1:1, such that a similar amount of computational time is spent on each. The attempted moves are accepted or rejected using the standard Metropolis algorithm.

As usual, a simulation starts with a large number of Monte Carlo steps (MCS) per monomer (typically 10^6) to equilibrate the system, followed by an even larger number (typ-

nearly 10^7) over which statistics are collected for various observables. Each observable, $\hat{O}$, is generally sampled once every 20 MCS per monomer. In order to reduce the computational effort, we employ Monte Carlo reweighting,[22,23] where $\hat{O}$ and the number of AB contacts, n_{AB}, are stored over one long simulation at some α_0. The ensemble average of $\hat{O}$ at α is then given by

$$\langle \hat{O} \rangle = \frac{\sum_i \hat{O}_i \exp\left(n_{AB,i}(\alpha - \alpha_0)\right)}{\sum_i \exp\left(n_{AB,i}(\alpha - \alpha_0)\right)} , \tag{3}$$

Not surprisingly, the reweighing will fail if α differs too much from α_0. Fortunately, reweighting works particularly well near a critical point, α_c, due to the broad distribution of configurations resulting from the critical fluctuations. To be absolutely safe, we repeat the simulation if our initial choice of α_0 differs from α_c by more than 0.5%.

III. RESULTS

Several different methods will be used to determine the critical points, α_c, for a series of polymerizations ranging from $N = 10$ to 320. Because the correlation length diverges as $\alpha \to \alpha_c$, the finite size of the simulation box will affect results no matter how large its width, $Lb/\sqrt{2} = 0.793L$, is relative to the average end-to-end length of the polymers, $R_0 = 1.384N^{1/2}$. Therefore, the only way to obtain α_c accurately is by employing finite-scaling techniques, whereby simulations are performed over a range of system sizes, L. The analysis turns out to be very sensitive to polymer density, and consequently L has to be strictly limited to values for which ρ_0 is exactly 0.8.

The usual way of accounting for finite-size effects is to plot the Binder (or fourth-order) cumulant[24]

$$U_{4,2} = 1 - \frac{\langle m^4 \rangle}{3\langle m^2 \rangle^2} , \tag{4}$$

for different L. Figure 1(a) shows sample results for $N = 40$, demonstrating the expected behavior where the curves cross at a fixed point, which in this case identifies the critical point as $\alpha_c = 0.0100057$. Figure 1(b) replots the data with the temperature axis scaled by $L^{1/\nu}$, where $\nu = 0.62997$ is the critical exponent of the correlation length for the 3D-Ising universality class. The near perfect collapse of the curves implies that the finite-size scaling is working properly. This scaling behavior will fail if L is too small, and indeed we have omitted our $L = 10$ results for this precise reason. Analogous plots for other values of N

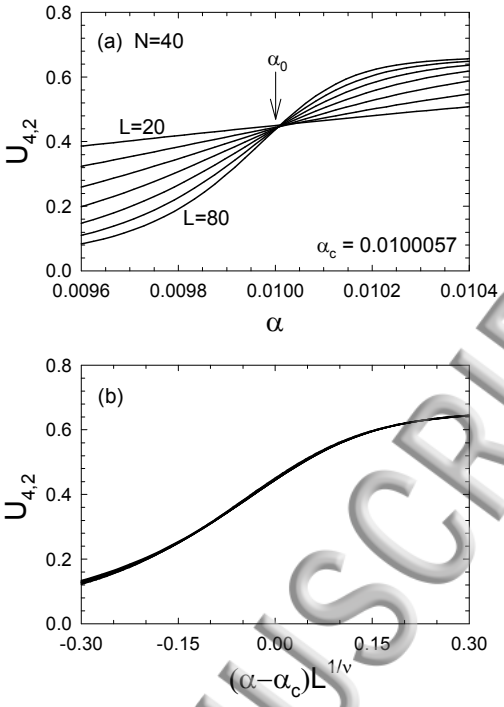

FIG. 1: (a) Fourth-order cumulant, $U_{4,2}$, as a function of $\alpha \equiv \epsilon_{AB}/k_BT$, calculated for $N = 40$ diblocks using simulation boxes of size $L = 20$ to 80 in steps of 10. The arrow denotes the point about which the MC reweighting was performed. (b) Results replotted with the temperature axis scaled by $L^{1/\nu}$, where $\nu = 0.62997$.

are shown in the Appendix, and the resulting critical points from this first method, $\alpha_c^{(1)}$, are listed in Table I.

Researchers often choose to examine the second-order cumulant

$$U_{2,1} = \frac{\langle m^2 \rangle}{\langle |m| \rangle^2} \ , \tag{5}$$

because it involves smaller moments of m, for which the statistics tend to be more accurate.[13] Figure 2 shows analogous plots to Fig. 1 using this alternative cumulant. There is again an excellent collapse of the curves in Fig. 2(b). The resulting critical points of this second approach, $\alpha_c^{(2)}$, which are tabulated in Table I for the various N, agree with those of the Binder cumulant to about four digits of accuracy. The agreement implies that the moments of m, including the fourth-order one, are all accurate, which testifies to the quality of our statistics.

To be absolutely certain that our simulation is behaving correctly, we consider one further

This manuscript was accepted by J. Chem. Phys. Click here to see the version of record.

TABLE I: Critical points, $\alpha_c^{(i)}$, determined from the fourth-order cumulant ($i = 1$), the second-order cumulant ($i = 2$), and the peak in the susceptibility ($i = 3$) for chains of different polymerization, N.

N	$\alpha_c^{(1)}$	$\alpha_c^{(2)}$	$\alpha_c^{(3)}$
10	0.036711	0.036702	0.036736
20	0.019379	0.019378	0.019378
40	0.010006	0.010004	0.010010
80	0.005092	0.005091	0.005096
160	0.002567	0.002567	0.002570
320	0.001288	0.001287	0.001291

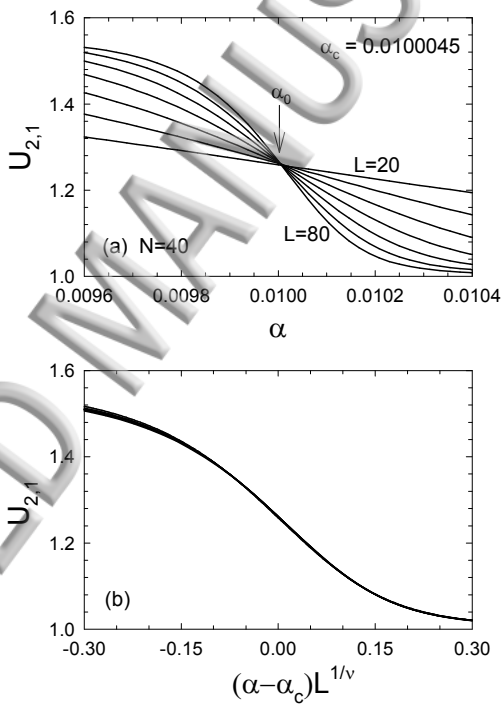

FIG. 2: Analogous plots to those of Fig. 1 for the second-order cumulant, $U_{2,1}$.

technique for finding the critical point that involves the susceptibility

$$\chi_{|m|} \equiv \frac{\partial}{\partial \mu} \langle |m| \rangle \Big|_{\mu=0} = \frac{n}{k_B T} \left(\langle m^2 \rangle - \langle |m| \rangle^2 \right) \ , \tag{6}$$

where μ is a chemical potential that couples to $|n_A - n_B|$. The first step is to locate the position of its maximum, $\alpha^{\max}$, for a series of system sizes, L, as demonstrated in Fig. 3(a)

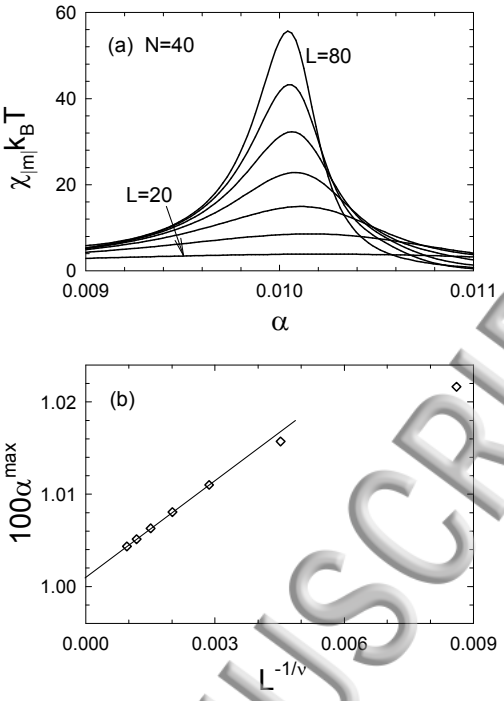

FIG. 3: (a) Susceptibility, $\chi_{|m|}$, as a function of α, calculated for $N = 40$ diblocks using simulation boxes of size $L = 20$ to 80 in steps of 10. (b) Position of the maximum, $\alpha^{\max}$, plotted as a function of system size scaled with the critical exponent ν. The straight line denotes the extrapolation to infinite L used to estimate α_c.

for polymers of length $N = 40$. The maximum is then plotted as a function of $L^{-1/\nu}$ and linearly extrapolated to $L \to \infty$, as shown in Fig. 3(b). In this case, the data does not become linear until $L \gtrsim 40$, whereas the cumulants began to scale accurately for $L \gtrsim 20$. Analogous plots for the larger N are shown in the Appendix. Although the predictions of this third method, $\alpha_c^{(3)}$, tabulated in Table I, are in good agreement with those obtained from the cumulants, we expect them to be less accurate in general given the need for larger system sizes.

So far, the scaling behavior appears to be consistent with the 3D-Ising universality class, in particular the value of ν. However, the fixed points of the two cumulants do not match the literature value, $U^*_{4,2} = 0.4652$,[25] and the value, $U^*_{2,1} = 1.23$, we obtained by simulating the 3D-Ising model (*i.e.*, $N = 1$ and $\rho_0 = 1$). Table II illustrates the discrepancy for $N = 40$ by tabulating the crossing points for subsequent pairs (L_1, L_2) of system sizes up to 7.2 times R_0. To within the resolution of our statistical accuracy, the U^*'s appear to plateau with no

TABLE II: Crossing points (α^*, U^*) of the fourth- and second-order cumulants in Figs. 1(a) and 2(a), respectively, for subsequent pairs of system sizes, L_1 and L_2.

L_1	L_2	$\alpha^*_{4,2}$	$U^*_{4,2}$	$\alpha^*_{2,1}$	$U^*_{2,1}$
10	20	0.010371	0.5042	0.010162	1.2323
20	30	0.010042	0.4568	0.010020	1.2557
30	40	0.010012	0.4479	0.010007	1.2599
40	50	0.010006	0.4451	0.010005	1.2606
50	60	0.010005	0.4445	0.010004	1.2617
60	70	0.010006	0.4451	0.010005	1.2608
70	80	0.010006	0.4452	0.010004	1.2613

hint of approaching the expected values. This same departure from the 3D-Ising values has, in fact, been observed in all polymer simulations,[12–14] and is attributed to the large number of intermolecular contacts among high molecular-weight polymers, which tends to suppress fluctuation effects. Consequently, as N increases, the apparent $U^*_{4,2}$ tends toward the mean-field value of 0.2705.[26] Indeed, the fixed point is reduced to 0.39 by the time $N = 320$; see Fig. 11 in the Appendix.

The polymeric nature of the system also tends to push certain critical exponents from their 3D-Ising value toward their mean-field value. This is evident from the behavior of the order parameter, $\langle|m|\rangle$. Deutsch and Binder[13] showed that its value at the critical point should scale as

$$\langle|m|\rangle_c \propto N^{\beta/\nu-1/2} L^{-\beta/\nu} \ . \tag{7}$$

Figure 4(a) confirms the power-law dependence on L, but finds that the *effective* exponent, $-\beta/\nu$, tabulated in Table III shifts away from the 3D-Ising value of -0.518 toward the mean-field value of -0.75 as N increases, as has been observed in previous studies.[13,14] Despite the shift in the exponent, Deutsch and Binder argued that $\langle|m|\rangle_c N^{1/2}$ should remain a function of L/N. Figure 4(b) shows that this scaling is indeed satisfied by our results, as was the case for their simulations.

Analogous behavior also occurs for the susceptibility, $\chi_{|m|}$. Deutsch and Binder[13] showed that the peak susceptibility from Fig. 3(a) should scale as

$$\chi^{\max}_{|m|} \propto N^{[-\gamma+4\beta-3\nu]/3\nu} L^{\gamma/\nu} \ . \tag{8}$$

This manuscript was accepted by J. Chem. Phys. Click here to see the version of record.

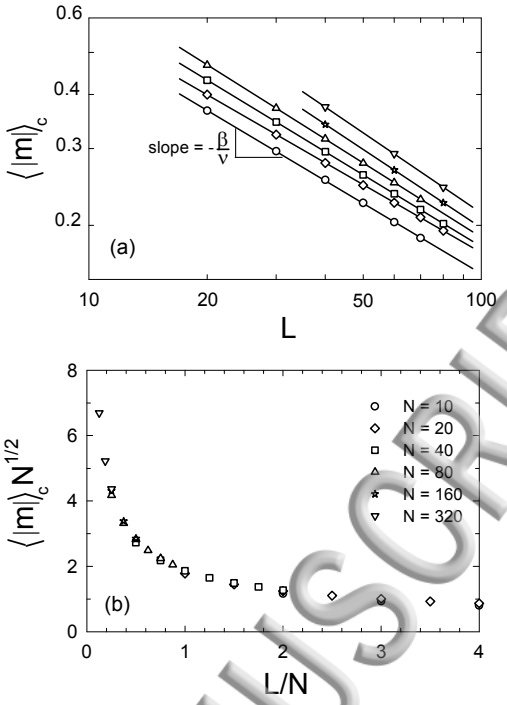

FIG. 4: Order parameter at the critical point, $\langle |m| \rangle_c$, as a function of system size, L, for different polymerizations, N. The slopes in the logarithmic plot (a) provide the ratio of critical exponents, β/ν, tabulated in Table III, and the collapse of the data in the linear plot (b) confirms the N dependence of Eq. (7).

TABLE III: Critical exponents extracted from Figs. 4(a), 5(a) and 6, for chains of different polymerization, N. The top row quotes their 3D-Ising values.

N	β/ν	γ/ν	$(2\beta+\gamma)/\nu$	$(1-\alpha)/\nu$
3D-Ising	0.518	1.964	3.000	1.413
10	0.539	1.974	3.052	1.411
20	0.520	1.950	2.990	1.410
40	0.548	1.919	3.016	1.410
80	0.568	1.898	3.034	1.413
160	0.597	1.826	3.021	1.413
320	0.614	1.822	3.050	1.413

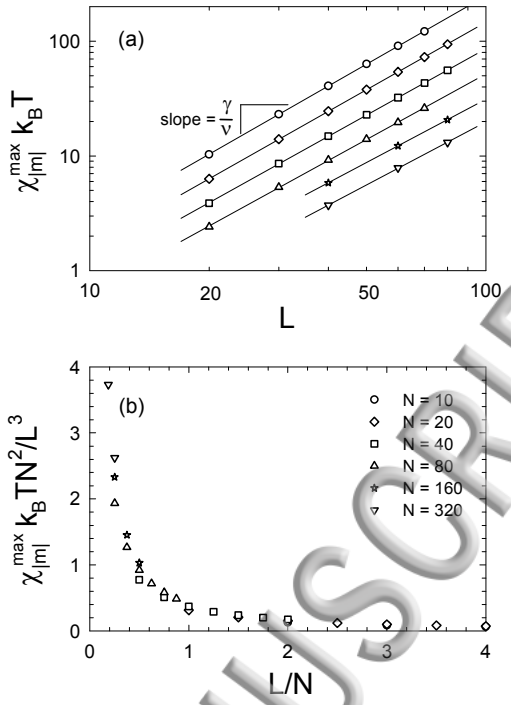

FIG. 5: Peak susceptibility, $\chi^{\max}_{|m|}$, as a function of system size, L, for different polymerizations, N. The slopes in the logarithmic plot (a) provide the ratio of critical exponents, γ/ν, tabulated in Table III, and the collapse of the data in the linear plot (b) confirms the N dependence of Eq. (8).

Figure 5(a) confirms the expected power-law dependence on L, but again the *effective* exponent, γ/ν, tabulated in Table III, shifts away from the 3D-Ising value of 1.964 as N increases.[13,14] Interestingly,γ/ν tracks the shift in β/ν so as to maintain the hyperscaling relation

$$2\frac{\beta}{\nu} + \frac{\gamma}{\nu} = 3 \; , \tag{9}$$

as confirmed in Table III as well as in the previous study of Deutsch and Binder. Given the hyperscaling, Deutsch and Binder argued that $\chi^{\max}_{|m|} N^2/L^3$ should depend only on the ratio L/N. Figure 5(b) confirms that our data collapses reasonably well when scaled in this manner, as was the case for the simulations of Deutsch and Binder.

We perform one further check of our results by examining the average internal energy at the critical point, which is expected to vary with system size, L, as[29]

$$\langle E \rangle_c = a_1 + a_2 L^{-(1-\alpha)/\nu} \; , \tag{10}$$

where α is the critical exponent corresponding to the heat capacity (not to be confused

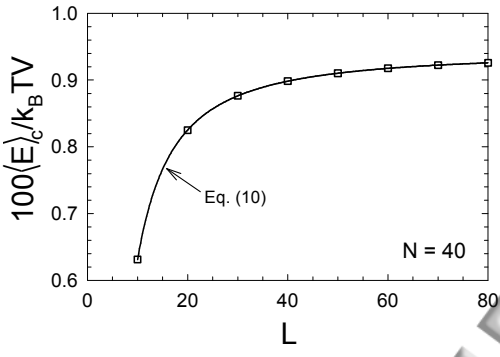

FIG. 6: Average internal energy at the critical point, $\langle E \rangle_c$, as a function of system size, L, for polymers of length $N = 40$. The curve is a fit to Eq. (10), which provides the value of $(1-\alpha)/\nu$ in Table III. Note: the conventional symbol for the critical exponent α should not be confused with our interaction parameter, $\alpha \equiv \epsilon_{\rm AB}/k_BT$.

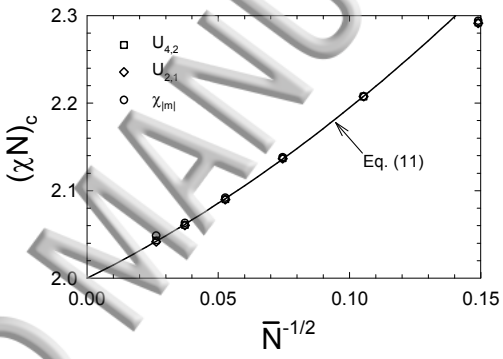

FIG. 7: The three estimates of the critical transitions from Table I plotted in terms of the nonlinear $\chi(\alpha)$ in Eq. (2) and the invariant polymerization index $\bar{N} = 4.506N$. The solid curve denotes the empirical fit in Eq. (11).

with the interaction strength $\alpha = \epsilon_{AB}/k_BT$). Figure 6 shows a three-parameter fit to our simulation data for $N = 40$, which gives $(1-\alpha)/\nu = 1.410$ in good agreement with the 3D-Ising value of 1.413. The exponents obtained from fitting the data for the other chain lengths, tabulated in Table III, exhibit similar agreement. Given that $\langle E \rangle$ needs to be evaluated at the critical point for this to work, the agreement is further evidence that our estimates of α_c are accurate.

Now that we are fully confident in the critical points tabulated in Table I, Fig. 7 plots the results in terms of $(\chi N)_c$ and the invariant polymerization index, $\bar{N}$, using the calibration

of $\chi(\alpha)$ in Eq. (2) and $\bar{N} = 4.506N$. The solid curve in Fig. 7 denotes a three-parameter fit,

$$(\chi N)_c = 2 + 1.47\bar{N}^{-1/2} + 4.8\bar{N}^{-1} \ , \tag{11}$$

to the $N \geq 20$ predictions from the two cumulant methods, which we consider slightly more accurate than the predictions from $\chi_{|m|}$. Note that the first parameter of the fit is actually 1.9998, which accurately rounds to the mean-field prediction of 2. This not only agrees with the fact that fluctuation effects vanish in the infinite molecular-weight limit, but also supports the belief that χ does not depend on molecular architecture, given that our χ in Eq. (2) was derived from simulations on diblock copolymer melts.

IV. DISCUSSION

Our finite-size scaling analysis seems to provide an impressive accuracy of four digits for the critical points, α_c. Of the different methods, we regard the two cumulant ones as the most accurate, given that the crossing points, α^*, plateau at relatively small system sizes. For instance, the crossing points in Table II for $N = 40$ approach a well-defined $\alpha^* = 1.0007$ once $L \gtrsim 40$. Nevertheless, one could be concerned by the significant deviations in the U^*'s from their universal 3D-Ising values, as has been the case in previous simulations.[12–14] Although the U^*'s must eventually approach their 3D-Ising values, the convergence proves to be incredibly slow, so much so that any evidence of it in Table II is obscured by our small statistical inaccuracies. Naturally, one might suspect a similar drift in α^* as $L \to \infty$, but it is, in fact, impossible for both quantities to simultaneously drift. As L increases, the slope $\frac{dU}{d\alpha}$ becomes steeper, constraining the possible deviation between α^* and α_c. By the time $L = 80$, the 4% deviation of $U^*_{4,2}$ from 0.465 in Table II bounds the deviation of α^* from α_c to approximately 0.003%. Thus, our value of α^* for $N = 40$ is an accurate estimate of α_c, even though the system remains too small to exhibit accurate 3D-Ising behavior. We assume a similar rapid convergence of $\alpha^* \to \alpha_c$ for our larger N values.

Although our finite-size scaling analysis showed excellent agreement with the 3D-Ising exponents $\nu = 0.62997$ and $\alpha = 0.11008$ in Figs. 1(b), 2(b), 3(b) and 6, one might be concerned by the sizable deviations in Figs. 4(a) and 5(a) from $\beta = 0.32642$ and $\gamma = 1.23707$. However, this was also observed by Deutsch and Binder.[13] Not only did they observe similar sized deviations in β and γ, their exponents continued to satisfy the hyperscaling relation,

Fig. (9), just as ours did. Deutsch and Binder later illustrated that the slopes of $\langle |m| \rangle_c$ and $\chi_{|m|}^{\max}$ in Figs. 4(a) and 5(a) do, in fact, cross over to the expected 3D-Ising values once the ratio of L/N is sufficiently large.[13,28] Given that the system size at which this happens scales as N, it simply becomes unfeasible to simulate systems of sufficient size once $N \gtrsim 20$.

The precision of our results is evident by the fact the data points in Fig. 7 for $N \geq 20$ are accurately described by the smooth three-parameter fit in Eq. (11), and more importantly by the fact the first coefficient agrees almost perfectly with the mean-field value. This bolsters our confidence that 1.47 is a reliable estimate for the slope of $(\chi N)_c$ versus $\bar{N}^{-1/2}$ in the $\bar{N} \to \infty$ limit [*i.e.,* the universal coefficient, c, in Eq. (1)]. However, one always needs to be cautious in extrapolating data, even when the fit appears very accurate. Indeed, we find significant variation in the fitting parameters depending on how many terms and how many values of N are included in the fit. For instance, the coefficient of the $\bar{N}^{-1/2}$ term varied by approximately ± 0.1, and therefore we round our estimate of c to 1.5. The estimated coefficient for the $\bar{N}^{-1}$ term is considerably less certain. In any case, its value will not be universal, given that it is sensitive to effects that depend on the number of molecules, $n \propto N^{-1}$, such as any specific details involving the chain ends. Nevertheless, one could hope that its value is reasonably similar among different systems.

The quality of our estimate, $c \approx 1.5$, is naturally dependent upon the accuracy with which we were able to determine α_c. It is likewise dependent on the accuracy with which $\bar{N} = 4.506N$ and $z_\infty = 4.897$ were determined in Ref. 18. However, in principle, the value of c is not affected by the nonlinearity of χ, that is the coefficients c_1 and c_2 in Eq. (2).[30] This is demonstrated in Fig. 8, where we compare $(\chi N)_c$ using the linear $\chi = z_\infty \alpha$ and the nonlinear $\chi(\alpha)$ in Eq. (2). Out of interest, we also plot the critical point using the effective $\chi = z(N)\alpha$ of Müller and Binder.[14] In this case, the value of c is affected. Based on the relation

$$\frac{z(N)}{z_\infty} \approx 1 + \left(\frac{6}{\pi}\right)^{3/2} \bar{N}^{-1/2} \tag{12}$$

derived by Morse and Chung,[8] it follows that c increases by $2(6/\pi)^{3/2}$ to a value of 6.75.[30] In light of these results, we can now understand the diverse conclusions reached by previous studies.

Let us start with the simulations of the bond fluctuation model (BFM).[13] The analysis by Müller,[15,16] using $\chi = z(N)\alpha$, predicted a value of $c \approx 4$ that is not terribly far off of 6.75.

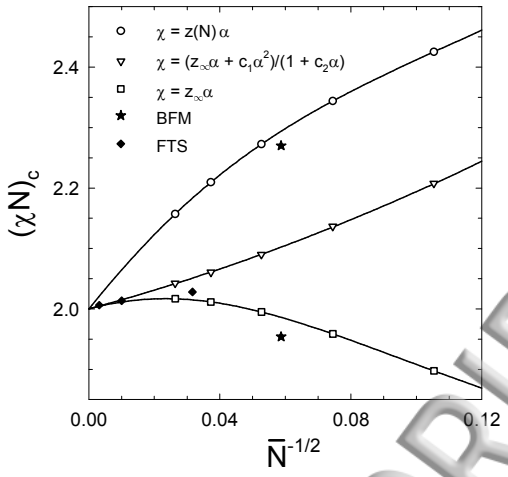

FIG. 8: Critical transition plotted using different definitions of the Flory-Huggins χ parameter. The solid curves show the transition as specified by the fit in Eq. (11).[30] Stars denote a simulation of the bond fluctuation model (BFM)[16,17] plotted using the two linear definitions of χ, and diamonds denote results from a field-theoretic simulation (FTS).[12]

On the other hand, the analysis by Qin and Morse,[9] using $\chi = z_\infty \alpha$, was unable to detect the $\bar{N}^{-1/2}$ scaling. As evident from the square symbols in Fig. 8, the same would have been true in our study had we just used $\chi = z_\infty \alpha$. With this definition, it becomes necessary to simulate far larger polymers in order to observe the $\bar{N}^{-1/2}$ scaling. To further illustrate the consistency with the BFM, Fig. 8 plots its critical point for $N = 64$ polymers.[16,17] The two points denoted by stars correspond to the linear definitions of χ with $z(N) = 2.44$ and $z_\infty = 2.10$.[31] They agree reasonably well with our simulations when the critical point is plotted in terms of $\chi = z(N)\alpha$ and $\chi = z_\infty \alpha$, respectively. Nevertheless, we should not expect a precise match, firstly because the comparison is not in terms of the nonlinear χ and secondly because the $\bar{N}^{-1}$ contributions to $(\chi N)_c$ are not universal.

The simulation by Detcheverry *et al.*[10] approximated the Gaussian chain model (GCM) by discretizing the polymer chains and smearing the interactions. To account for these modifications, they needed to define an effective χ parameter, which was obtained by matching the chemical potential for the exchange of A and B molecules to that of mean-field theory. However, this was done at finite values of N, and thus it results in an N-dependent χ. Indeed, previous simulations[14,16] have shown that this definition approximately matches $\chi = z(N)\alpha$. This is presumably the reason for their large estimate of $c \approx 10$, which is not

ing different from 6.75.

The critical points from the field theoretic simulations (FTS) of Spencer and Matsen[12] are also shown in Fig. 8. Results for the two largest molecules, $\bar{N} = 10^4$ and 10^5, agree well with Eq. (11), but the data point for $\bar{N} = 10^3$ starts to deviate significantly. Spencer has repeated some of the simulation runs to ensure that the deviation is statistically accurate.[32] It is important to note that the FTS has to contend with an ultraviolet divergence as the spatial resolution, Δ, of the grid upon which the fluctuating fields are represented becomes finer. The effect of the divergence is to reduce the incompatibility of the A and B molecules,[33] and as such it can be removed by defining

$$\chi = \left(1 - \frac{2.332 R_0}{\bar{N}^{1/2}\Delta}\right)\chi_b \tag{13}$$

where χ_b is the bare interaction parameter used in the simulation (*i.e.*, the equivalent of α). We suspect that the deviation from Eq. (11) is due to the fact that the effective χ in Eq. (13) is linear in the bare χ_b, which is akin to using the linear χ in particle-based simulations. Indeed, the FTS results are a closer match to the curve for $\chi = z_\infty \alpha$.

Although we can rationalize all the previous simulation results, it would be extremely useful to have accurate predictions of $(\chi N)_c$ for other models in terms of the nonlinear χ in order to confirm the universality of the $\bar{N}^{-1/2}$ fluctuation correction and to gauge the importance of the $\bar{N}^{-1}$ contributions. This could be achieved by simply applying the Morse calibration of the χ parameter to the two variants of the BFM simulated by Deutsch and Binder.[13] Alternatively, there are several other models that have already been calibrated in Ref. 18, just waiting to be applied to binary blends. Indeed, Mysona and Morse are in the process of doing so, and we have been informed that their results appear to be consistent with ours.[34]

V. CONCLUSIONS

Precise estimations for the critical point, α_c, of symmetric A+B homopolymer blends were obtained for a simple lattice model using finite-size scaling techniques. Our first two estimations were obtained from the fixed points, (α^*, U^*), of the fourth- and second-order cumulants of $m = (n_A - n_B)/(n_A + n_B)$ in Eqs. (4) and (5), respectively. In both cases, α^* provided accurate estimates of α_c for relatively small system sizes, L. Our third approach

extrapolated the peak position, $\alpha^{\max}$, of the susceptibility $\chi_{|m|}$ in Eq. (8) to $L \to \infty$. This provided a consistent estimate of α_c, although the finite-size scaling, $\alpha^{\max} \propto L^{-1/\nu}$, required somewhat larger system sizes. For this reason, we attributed greater accuracy to the cumulant methods.

The finite-size scaling analysis was largely consistent with the 3D-Ising universality class. For instance, the impressive collapse of the cumulants in Figs. 1(b) and 2(b) and the linearity of $\alpha^{\max}$ in Fig. 3(b) was achieved with the 3D-Ising value of ν. Furthermore, the dependence of the internal energy at the critical point, $\langle E \rangle_c$, with system size in Fig. 6 also scaled with the expected 3D-Ising exponent. However, the *effective* critical exponents, β and γ, determined from Figs. 4(a) and 5(a), respectively, deviated from the 3D-Ising values toward the mean-field values as N increased, but in such a way so as to maintain the hyperscaling relation in Eq. (9). This deviation has been observed before,[13,14] and results due to the suppression of fluctuation effects as $\bar{N} \to \infty$.[27,28] To achieve 3D-Ising behavior requires system sizes beyond what is computationally feasible. Another consequence of the limited system sizes is that the *effective* fixed-points of the cumulants, U^*, shift toward the mean-field values.[12–14] Nevertheless, this is expected to have a negligible impact on the convergence of α^*, and therefore should not compromise our estimates of α_c.

Using a previous calibration of our model for diblock copolymer melts,[18] Fig. 7 plots the critical points in terms of $(\chi N)_c$ and $\bar{N}$. The fit in Eq. (11) to the simulation data illustrates that the dominant fluctuation correction scales as $\bar{N}^{-1/2}$ and that the mean-field result of 2 is recovered in the infinite molecular-weight limit. Given that our χ is determined from diblock copolymer melts, the latter result strongly supports the notion that χ is independent of architecture. The fit also provides a reliable estimate, $c \approx 1.5$, for what is believed to be the universal coefficient in Eq. (1). Not only does the value agree with recent field-theoretic simulations (FTS),[12] we are also able to rationalize the previous simulations of the bond fluctuation model (BFM).[13] A previous lack of evidence for the $\bar{N}^{-1/2}$ scaling can be attributed to the use of $\chi = z_\infty \alpha$,[9] and the previous prediction of a much larger c can be attributed to the use of $\chi = z(N)\alpha$.[15,16] Although our findings are reasonably consistent with the present literature, it will be necessary to test other simulation models using the nonlinear χ to truly establish the universality of c.

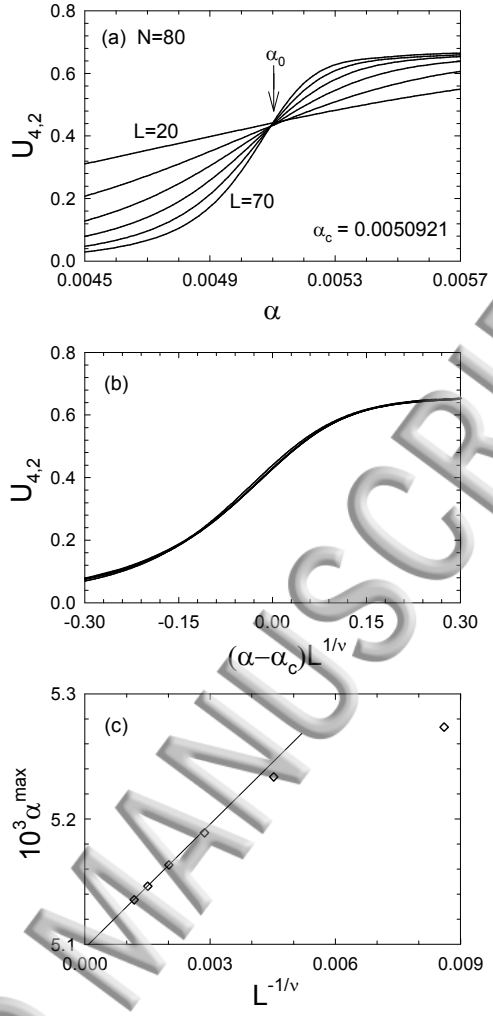

FIG. 9: Finite-size scaling analysis for $N = 80$ polymers using $L = 20$ to 70 in steps of 10. (a) Plots the Binder cumulant, (b) replots the results with a scaled temperature axis, and (c) extrapolates the peak of the susceptibility to infinite L. The arrow in (a) denotes the point used for the MC reweighting.

Acknowledgments

We thank Russell Spencer for checking the accuracy of the FTS results for $\bar{N} = 10^3$ in Ref. 12. This work was funded through a collaboration with the University of Minnesota's Center for Sustainable Polymers (CHE-1413862), and computer resources were provided by SHARCNET of Compute Canada.

This manuscript was accepted by J. Chem. Phys. Click here to see the version of record.

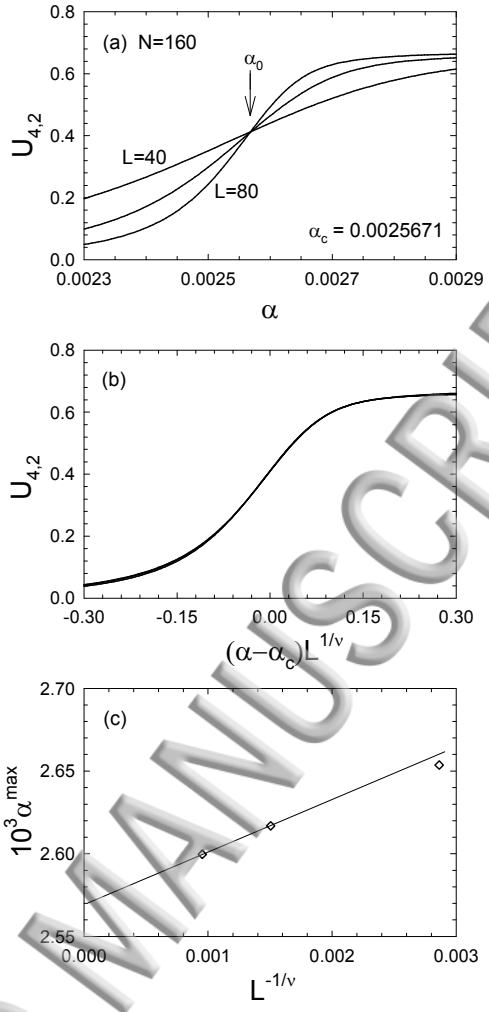

FIG. 10: Analogous finite-size scaling analysis to that of Fig. 9, but for $N = 160$ polymers using $L = 40$, 60 and 80.

Appendix

The Results section focused on our simulations at the modest polymerization of $N = 40$, for which we were able to consider a wide range of system sizes extending up to $7.2R_0$. Here we show analogous results to those of Figs. 1 and 3(b) for the $N = 80$, 160 and 320 polymers.

Figure 9 displays the finite-scaling analysis used to obtain the estimates of the critical point for $N = 80$ in Table I. The top plot (a) shows the Binder cumulants evaluated for a series of system sizes, $L = 20$, 30, 40,..., 70, from which the fixed point provides the first estimate, $\alpha_c^{(1)}$. The next plot (b) illustrates the collapse of the curves, when the temperature

This manuscript was accepted by J. Chem. Phys. Click here to see the version of record.

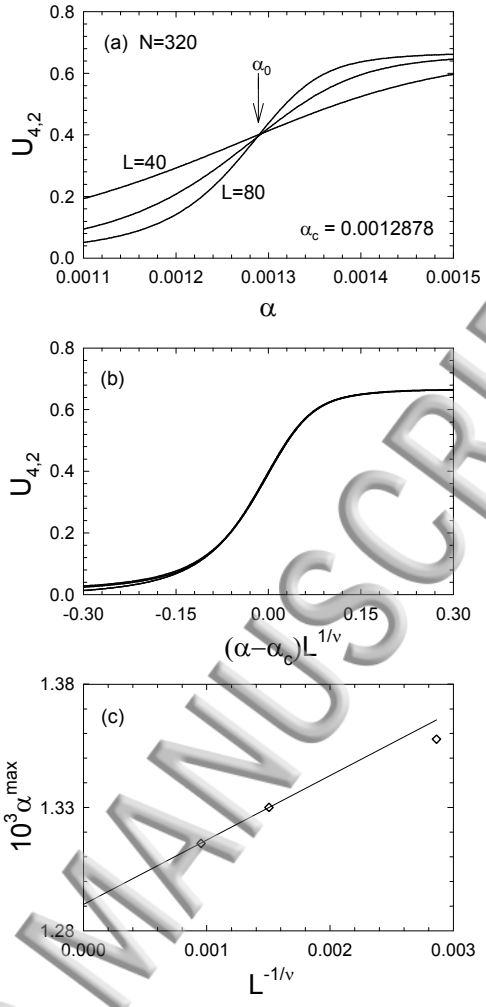

FIG. 11: Analogous finite-size scaling analysis to that of Fig. 9, but for $N = 320$ polymers using $L = 40$, 60 and 80.

axis is scaled by $L^{1/\nu}$ with the 3D-Ising critical exponent, $\nu = 0.62997$. Evidently, the scaling is not accurate for the smallest system size of $L = 20$; the curve is slightly above the fixed point in plot (a) and does not collapse on top of the other curves in plot (b). Note that the second-order cumulant (not shown) performs similarly and provides a nearly identical estimate, $\alpha_c^{(2)}$. The final estimate, $\alpha^{(3)}$, is obtained in plot (c) by extrapolating the peak position, $\alpha^{\max}$, of the susceptibility to infinite L. In this case, $L \gtrsim 40$ is required for the finite-size scaling to become accurate.

Figure 10 repeats the finite-scaling analysis for $N = 160$ polymers. With these larger molecules, the system size needs to be a multiple of 20 in order to strictly maintain a polymer density of $\rho_0 = 0.8$. We know from the $N = 80$ results that the scaling will not be accurate

for $L = 20$, and furthermore it is computationally unfeasible to consider system sizes as large as $L = 100$. Therefore, we are limited to $L = 40$, 60 and 80. Nevertheless, the three cumulants in Fig. 10(a) produce an unambiguous fixed point, and they accurately collapse in Fig. 10(b) when scaled with respect to $L^{1/\nu}$. As for the susceptibility, L needs to be about $\sqrt{2}$ times larger than for the $N = 80$ polymers in Fig. 9(c). Although system sizes of $L = 60$ and 80 should be sufficient for the finite-size scaling to work, $L = 40$ is undoubtedly too small. Indeed, the three data points in Fig. 10(c) do not lie in a straight line, but the largest two systems sizes do, in fact, extrapolate to a value $\alpha_c^{(3)}$ consistent with the predictions of the two cumulant methods.

The results for our largest $N = 320$ polymers are shown in Fig. 11. The system size is again limited to $L = 40$, 60 and 80. Based on our results for the shorter chains, $L = 60$ and 80 should be more than adequate for the cumulant method, and thus their crossing point is expected to provide an accurate estimate for α_c. This expectation is well supported by the fact that the $L = 40$ curve comes rather close to the same crossing point and also by the fact that all three cumulants collapse reasonably well in Fig. 11(b). As for the susceptibility method, $L = 40$ is definitely too small and even $L = 60$ is somewhat questionable. Therefore, we might suspect that the linear extrapolation of $L = 60$ and 80 would fail to provide an accurate estimate of α_c, but in fact $\alpha_c^{(3)}$ is close to the $\alpha_c^{(1)}$ and $\alpha_c^{(2)}$ obtained from the cumulant methods.

[1] P. J. Flory, J. Chem. Phys. **10**, 51 (1942).

[2] M. L. Huggins, J. Phys. Chem. **46**, 151 (1942).

[3] P. Knychała, K. Timachova, M. Banaszak and N. P. Balsara, Macromolecules **50**, 3051 (2017).

[4] G. H. Fredrickson, *The Equilibrium Theory of Inhomogeneous Polymers* (Oxford University Press, New York, 2006).

[5] M. W. Matsen, in *Soft Matter: Polymer Melts and Mixtures*, edited by G. Gompper and M. Schick (Wiley-VCH, Weinheim, 2006).

[6] Z.-G. Wang, J. Chem. Phys. **117**, 481 (2002).

[7] P. Grzywacz, J. Qin, and D. C. Morse, Phys. Rev. E **76**, 061802 (2007).

[8] D. C. Morse and J. K. Chung, J. Chem. Phys. **130**, 224901 (2009).

[9] J. Qin and D. C. Morse, J. Chem. Phys. **130**, 224902 (2009).

[10] F. A. Detcheverry, D. Q. Pike, P. F. Nealey, M. Müller and J. J. de Pablo, Phys. Rev. Lett. **102**, 197801 (2009).

[11] G. H. Fredrickson, V. Ganesan and F. Drolet, Macromolecules **35**, 16 (2002).

[12] R. K. W. Spencer and M. W. Matsen, Macromolecules **49**, 6116 (2016).

[13] H. P. Deutsch and K. Binder, Macromolecules **25**, 6214 (1992).

[14] M. Müller and K. Binder, Macromolecules **28**, 1825 (1995).

[15] M. Müller, Macromol. Theory Simul. **8**, 343 (1999).

[16] M. Müller, in *Soft Matter: Polymer Melts and Mixtures*, edited by G. Gompper and M. Schick (Wiley-VCH, Weinheim, 2006).

[17] M. Müller and J. J. de Pablo, Lect. Notes Phys. **703**, 76 (2006).

[18] J. Glaser, P. Medapuram, T. M. Beardsley, M. W. Matsen and D. C. Morse, Phys. Rev. Lett. **113**, 068302 (2014).

[19] P. Medapuram, J. Glaser and D. C. Morse, Macromolecules **48**, 819 (2015).

[20] T. M. Beardsley and M. W. Matsen, Phys. Rev. Lett. **117**, 217801 (2016).

[21] O. N. Vassiliev and M. W. Matsen, J. Chem. Phys. **118**, 7700 (2003).

[22] A. M. Ferrenberg and R. H. Swendsen, Phys. Rev. Lett. **61**, 2635 (1988).

[23] A. M. Ferrenberg and R. H. Swendsen, Phys. Rev. Lett. **63**, 1195 (1989).

[24] K. Binder, Phys. Rev. Lett. **47**, 693 (1981).

[25] H. W. J. Blöte, E. Luijten and J. R. Heringa, J. Phys. A: Math. Gen. **28**, 6289 (1995).

[26] E. Luijten and H. W. J. Blöte, Phys. Rev. Lett. **76**, 1557 (1996).

[27] H. P. Deutsch and K. Binder, Europhys. Lett. **18**, 667 (1992).

[28] H. P. Deutsch and K. Binder, J. Phys. II France **3**, 1049 (1993).

[29] M. Hasenbusch and K. Pinn, J. Phys. A: Math Gen. **31**, 6157 (1998).

[30] To switch to the linear definitions of χ, we substitute Eq. (2) into Eq. (11) and solve for α_c as a function of $\bar{N}$. From that $(\chi N)_c = z_\infty \alpha_c N$ follows immediately, and then $(\chi N)_c = z(N)\alpha_c N$ is obtained using Eq. (12), which is shown to be accurate in Ref. 18.

[31] The BFM results for $N = 64$ are plotted using the more accurate estimate of $\bar{N} = 290$ from Ref. 9

[32] R. K. W. Spencer (private communication).

[33] M. O. de la Cruz, S. F. Edwards and I. C. Sanchez, J. Chem. Phys. **89**, 1704 (1988).

[34] D. C. Morse (private communication).

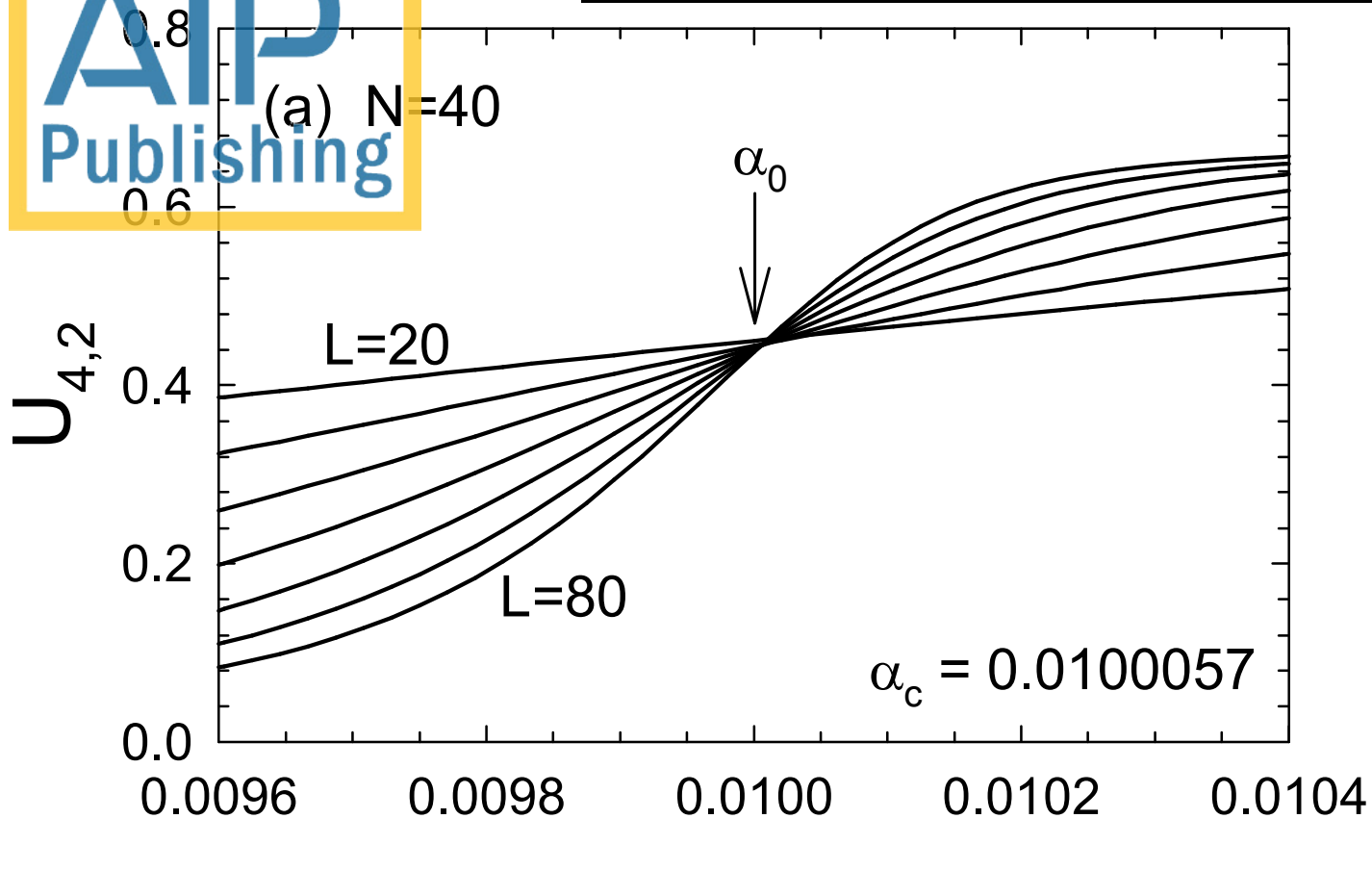

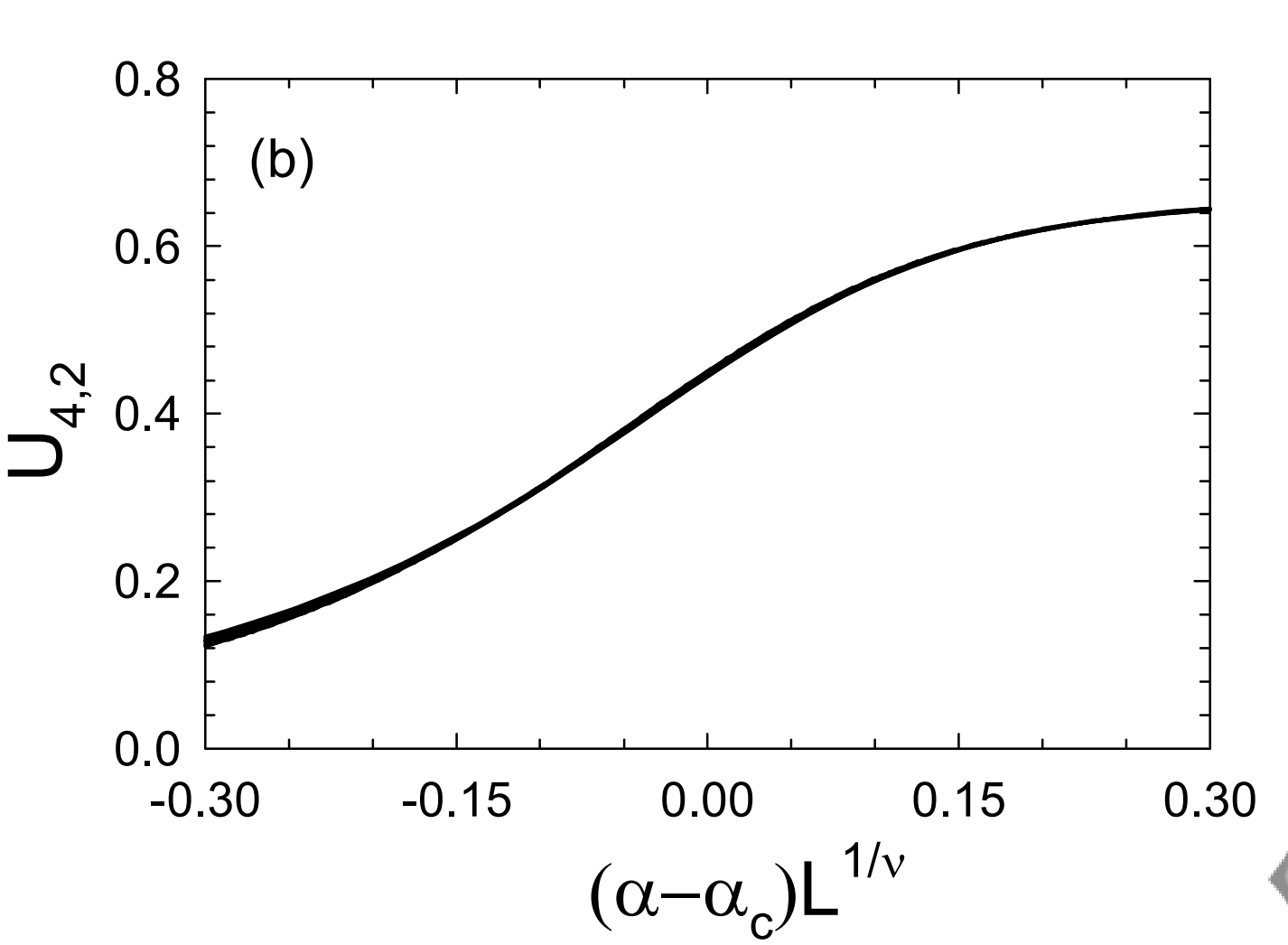

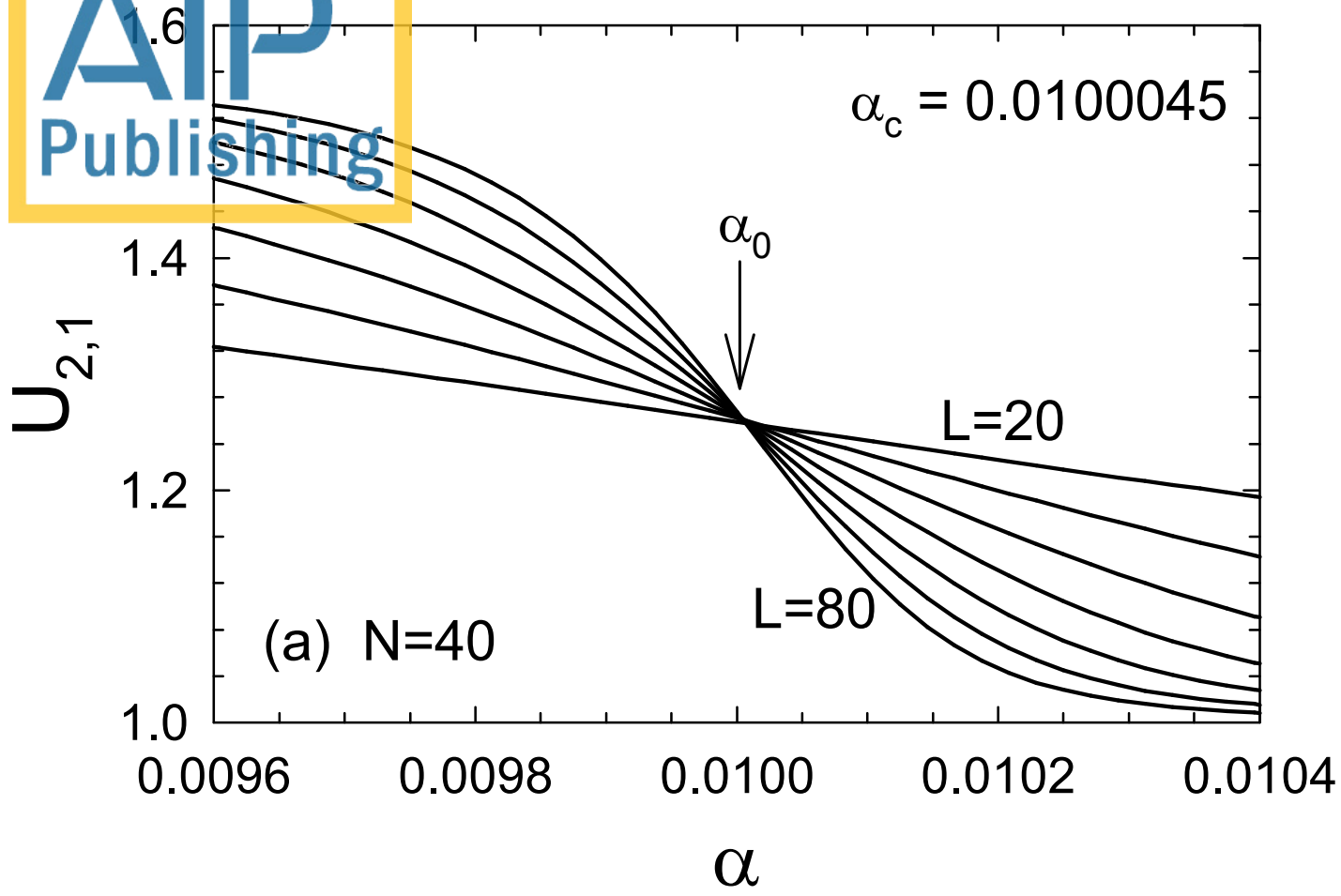
α_c = 0.0100045
α_0
L=20
L=80
(a) N=40
$U_{2,1}$
1.6
1.4
1.2
1.0
0.0096
0.0098
0.0100
0.0102
0.0104
α

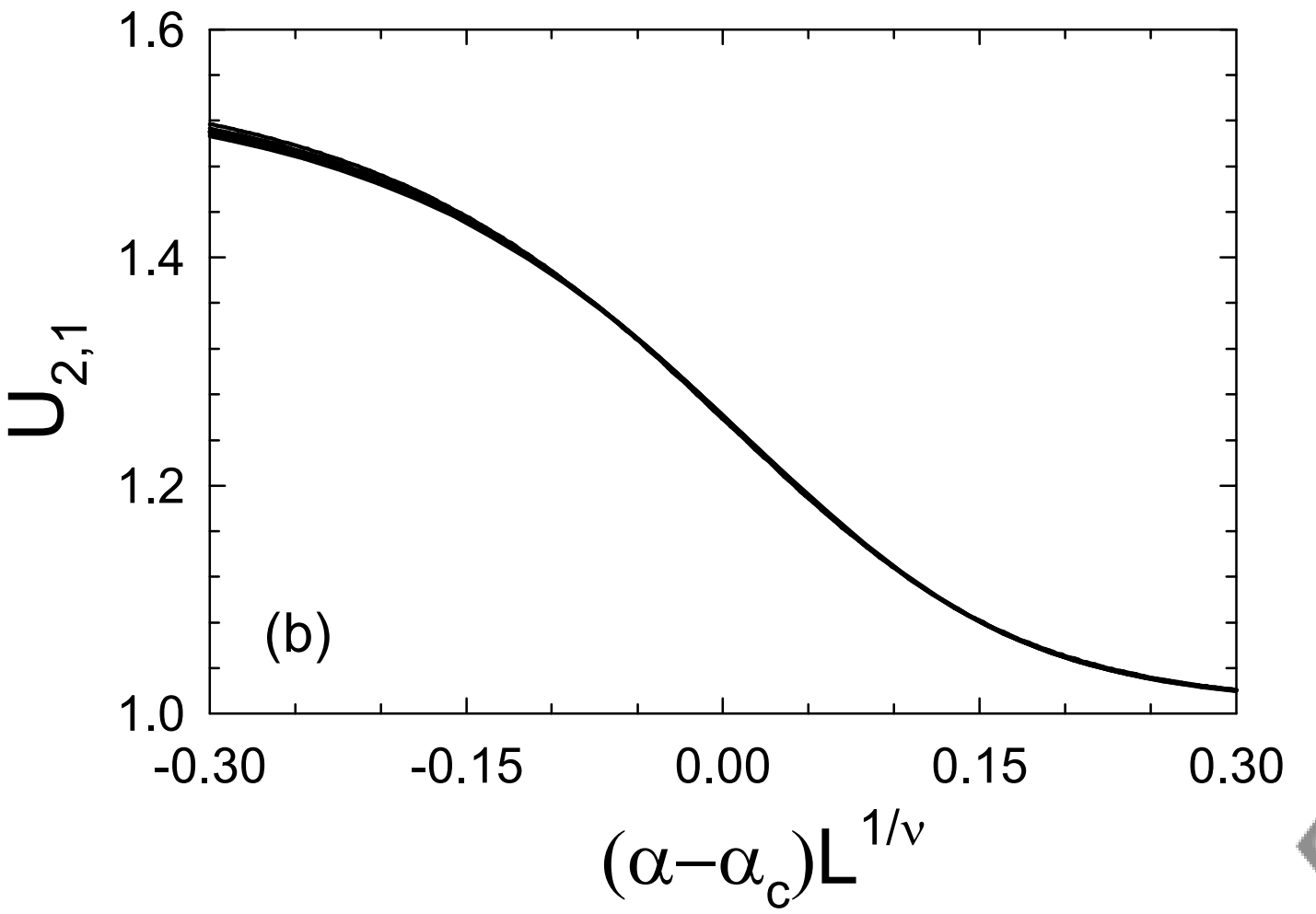
(b)
$U_{2,1}$
1.6
1.4
1.2
1.0
-0.30
-0.15
0.00
0.15
0.30
$(\alpha-\alpha_c)L^{1/\nu}$

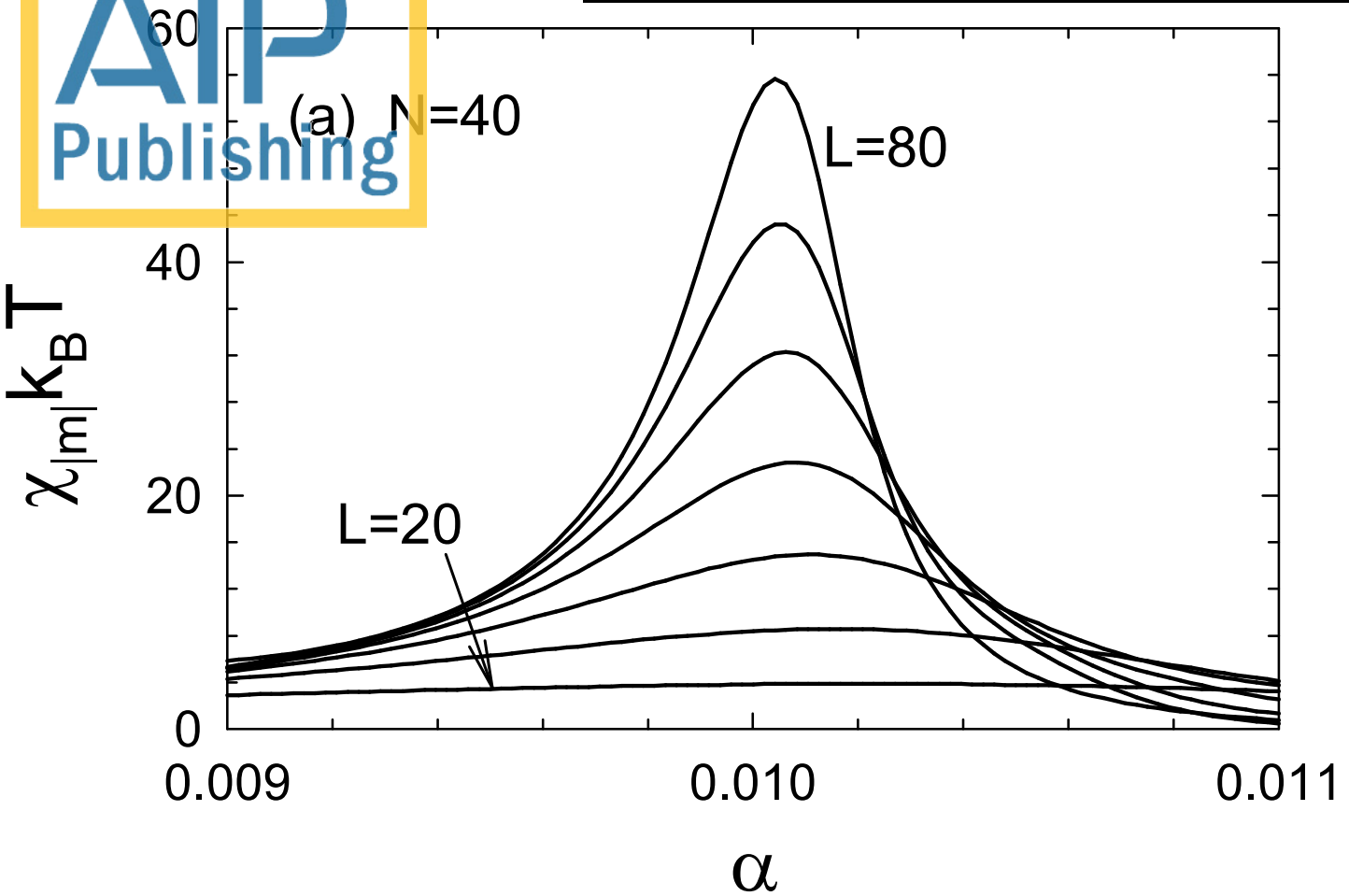

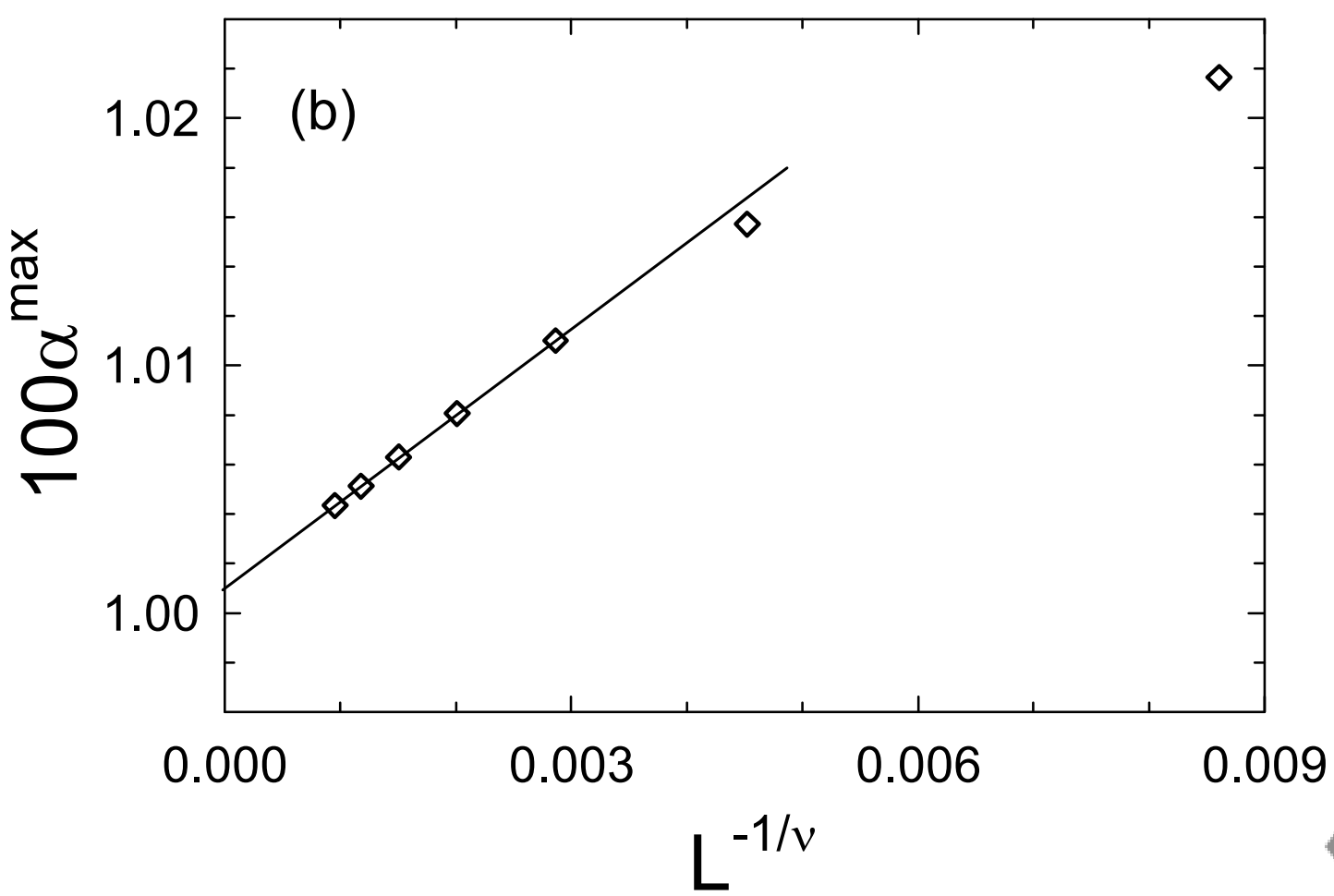

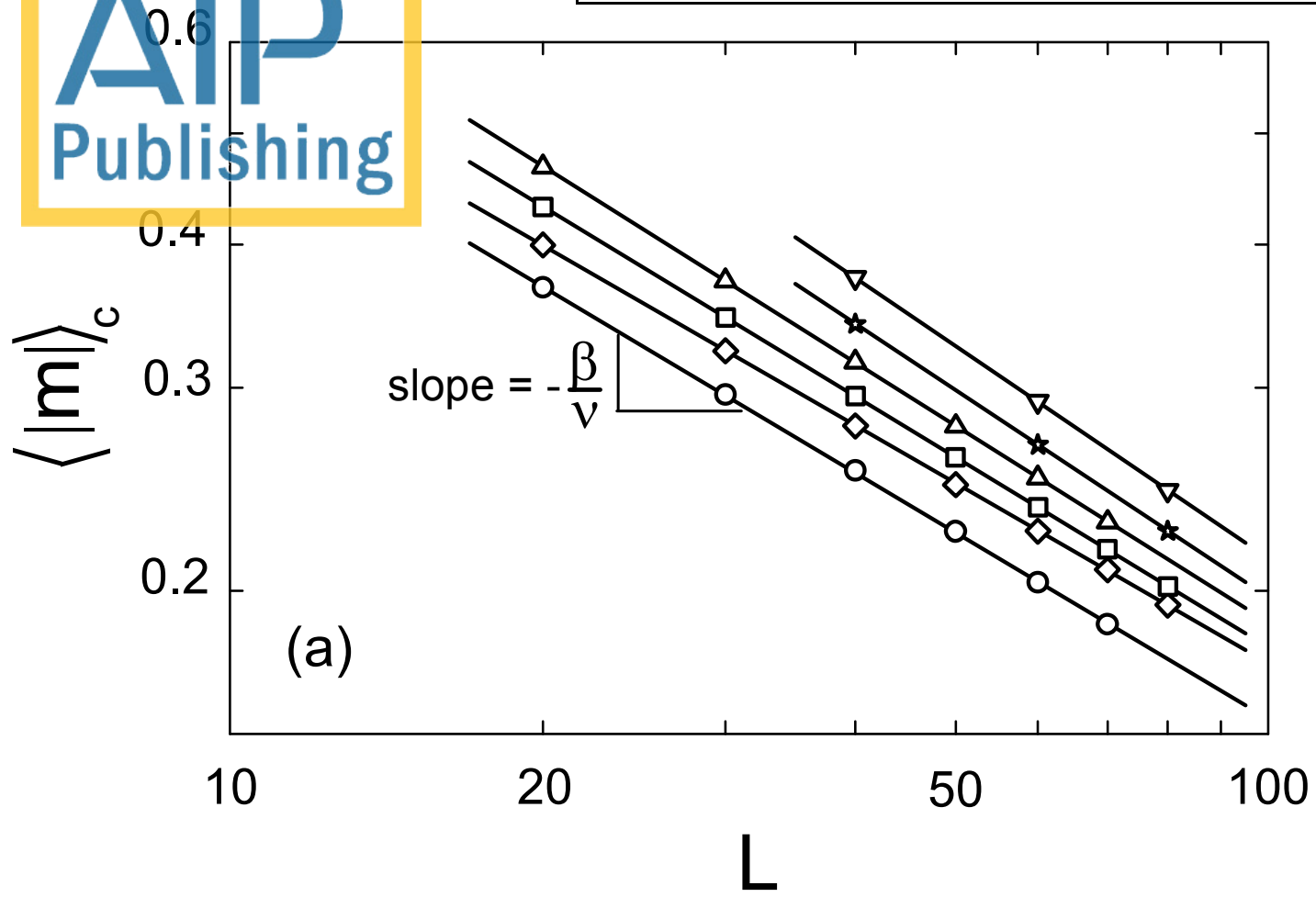

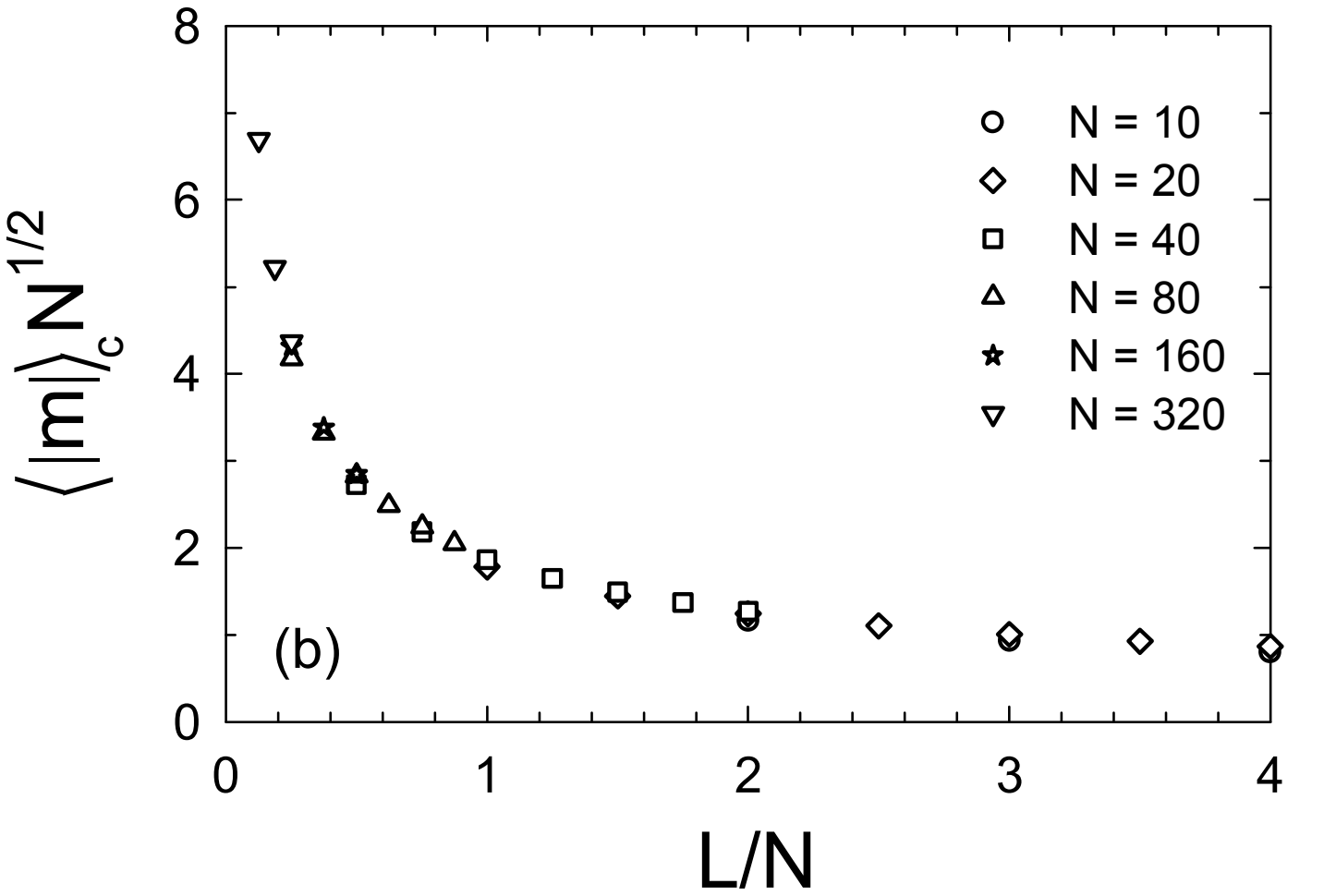

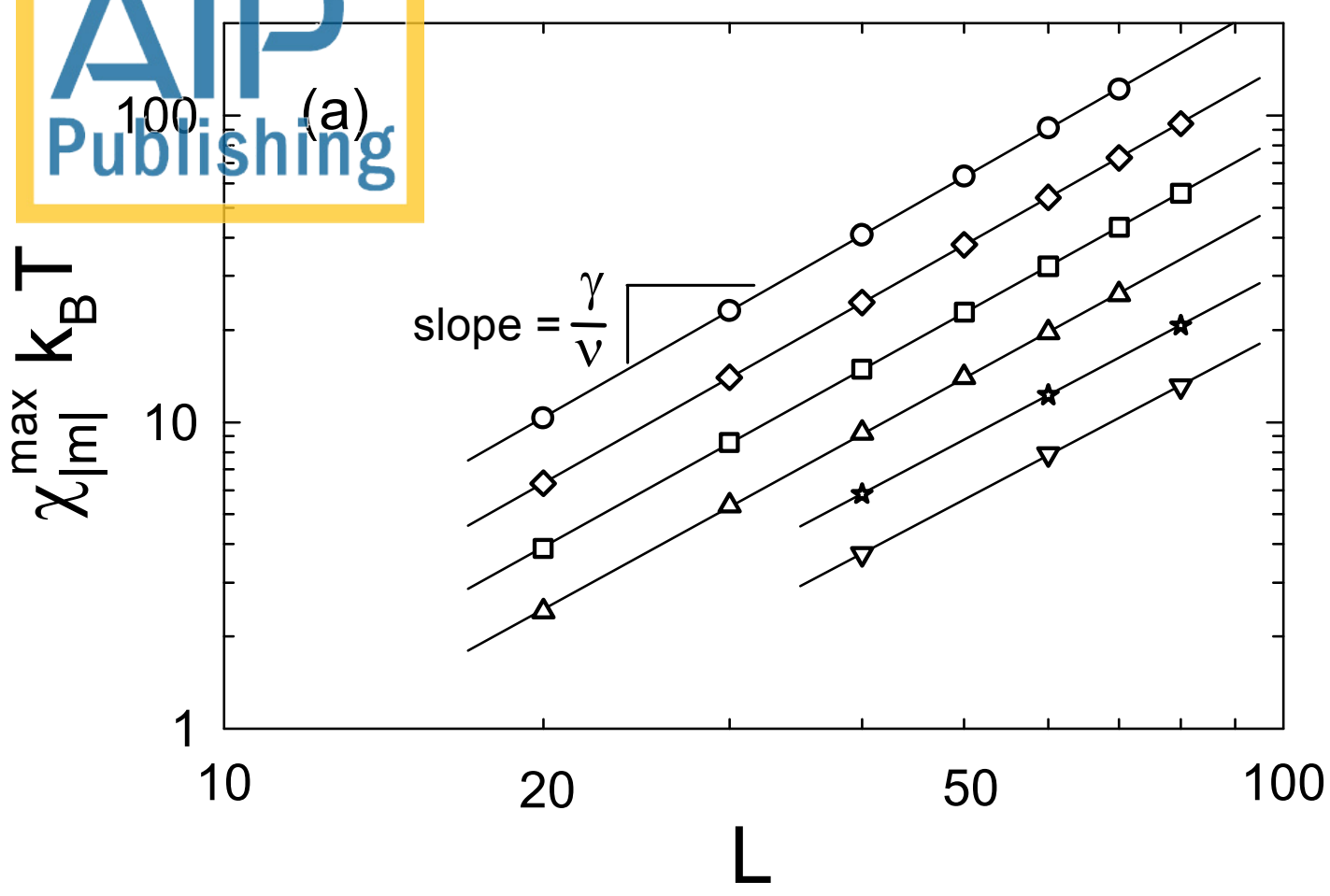

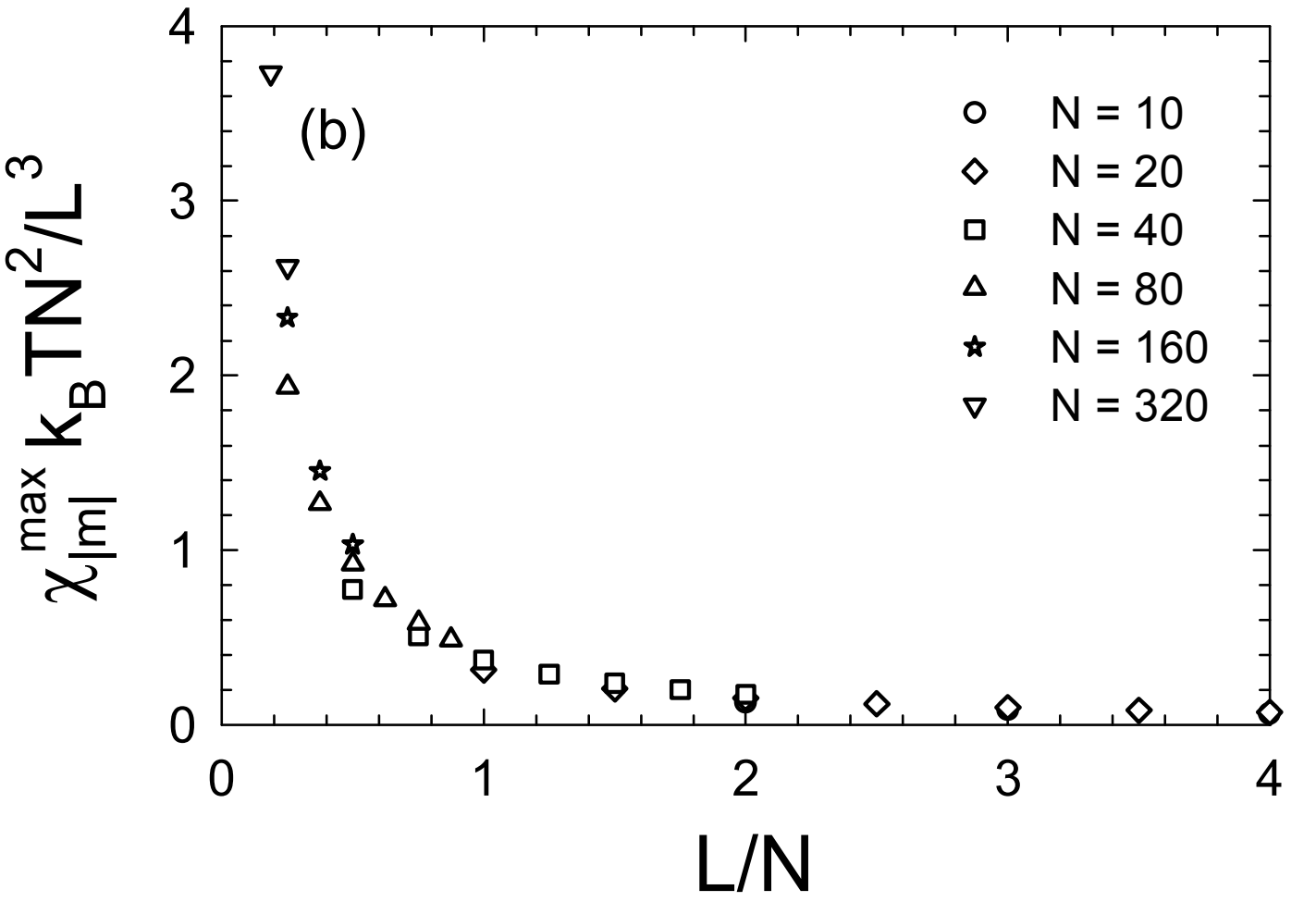

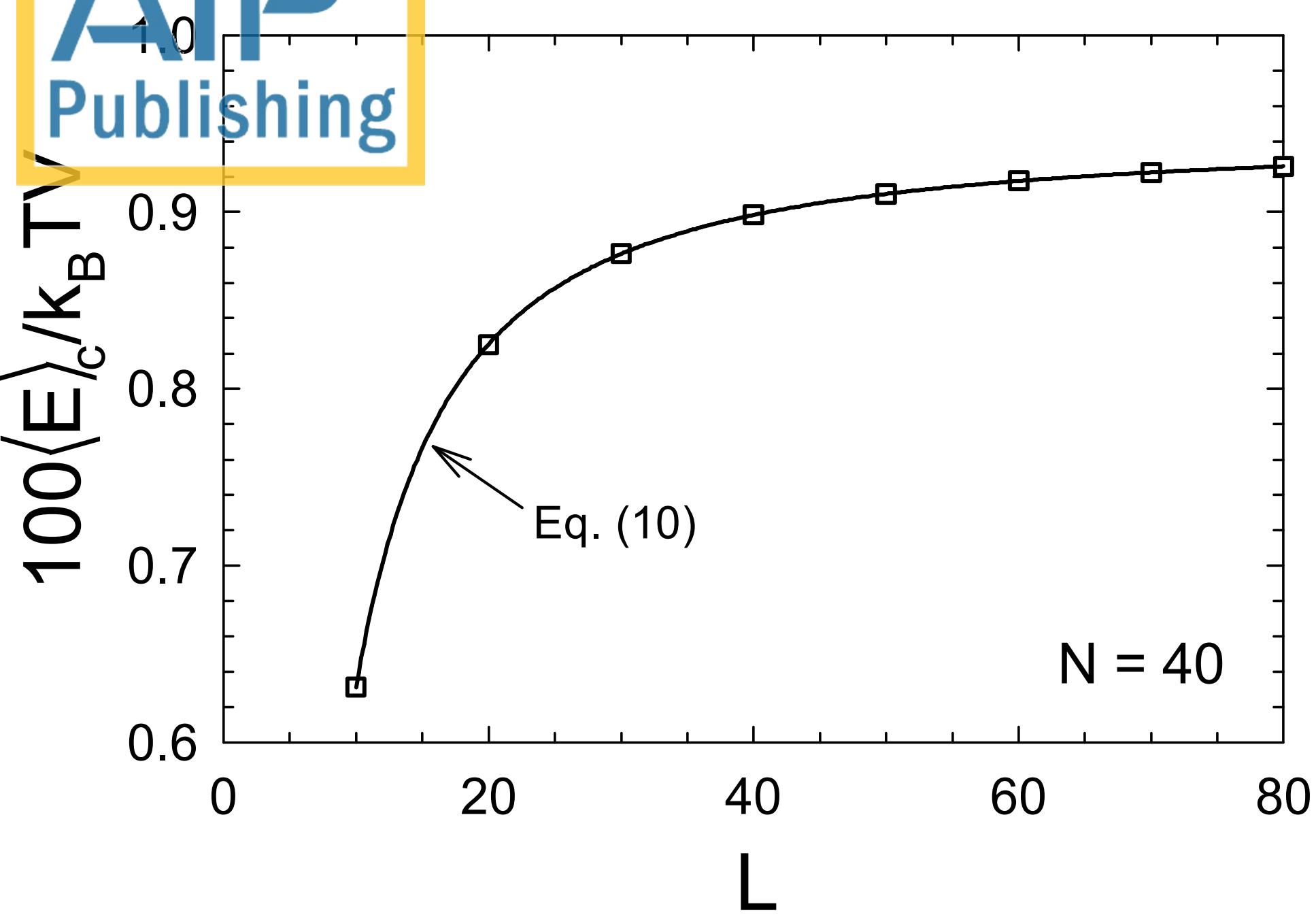
1.0
0.9
0.8
0.7
0.6
$100\langle E\rangle_c/k_BTV$
0
20
40
60
80
L
Eq. (10)
N = 40

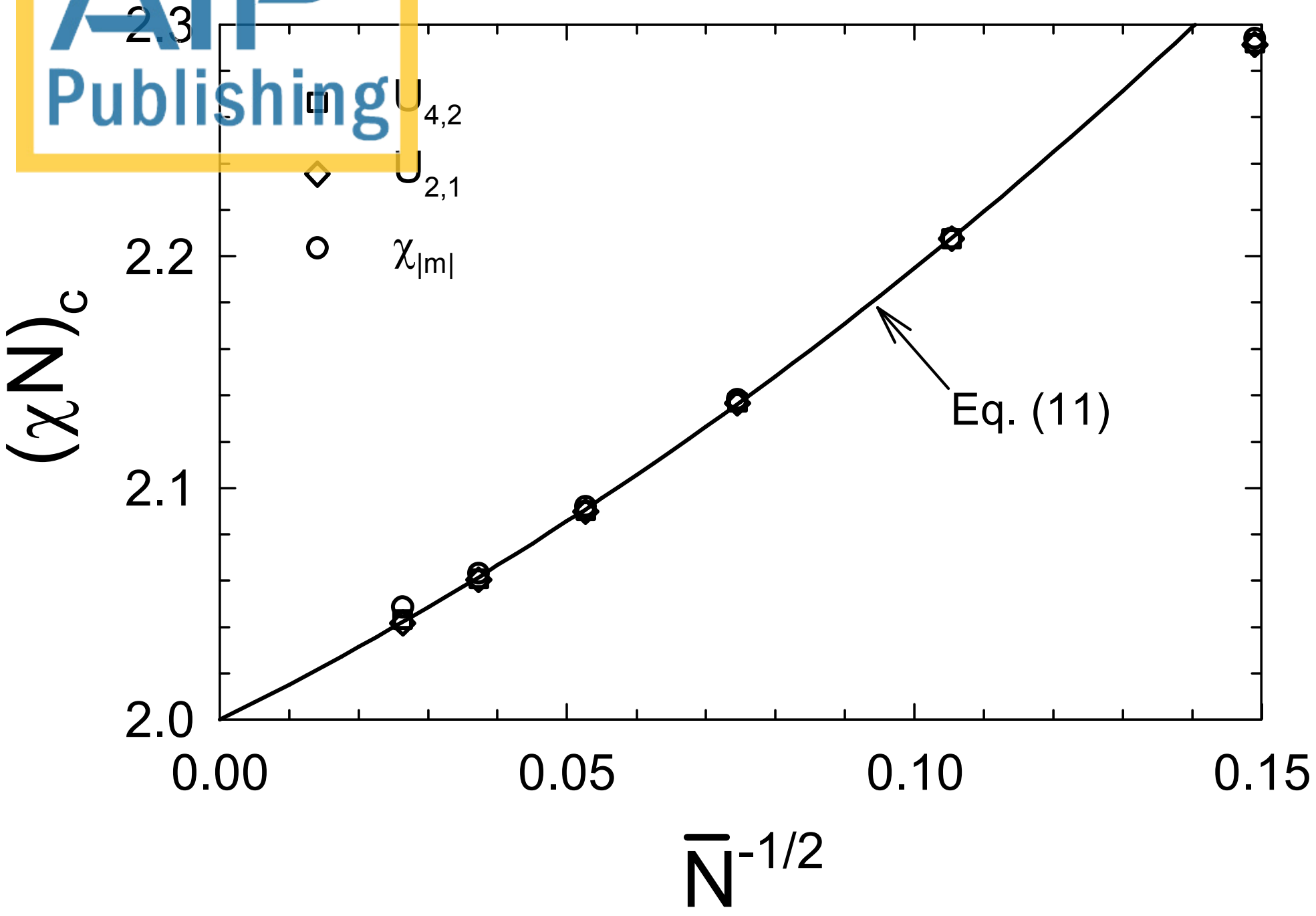
2.3
2.2
2.1
2.0
$(\chi N)_c$
$U_{4,2}$
$U_{2,1}$
$\chi_{|m|}$
Eq. (11)
0.00
0.05
0.10
0.15
$\bar{N}^{-1/2}$